

11

Betatron

The betatron [D.W. Kerst, Phys. Rev. **58**, 841 (1940)] is a circular induction accelerator used for electron acceleration. The word betatron derives from the fact that high-energy electrons are often called β -particles. Like the linear induction accelerator, the betatron is the circuit equivalent of a step-up transformer. The main difference from the linear induction accelerator is that magnetic bending and focusing fields are added to confine electrons to circular orbits around the isolation core. The beam acts as a multi-turn secondary. A single-pulsed power modulator operating at a few kilovolts drives the input; the output beam energy may exceed 100 MeV. The maximum electron kinetic energy achieved by betatrons is about 300 MeV. The energy limit is determined in part by the practical size of pulsed magnets and in part by synchrotron radiation.

General principles of the betatron are introduced in Section 11.1. The similarities between the power circuits of the linear induction accelerator, the recirculating induction linear accelerator, and the betatron are emphasized. An expression is derived for the maximum energy from a betatron; neglecting radiation, the limit depends only on the properties of the ferromagnetic core.

Two areas of accelerator physics must be studied in detail in order to understand the betatron; the theory of particle orbits in a gradient-type magnetic field and properties of magnetic circuits. Regarding orbits, the simple theory of betatron oscillations introduced in Section 7.3 must be extended. The amplitude of transverse-orbit oscillations and conditions for constant main-orbit radius must be determined for highly relativistic particles in a slowly changing magnetic field. Section 11.2 treats main orbit equilibria. The main orbit in the betatron has a constant radius

Betatron

during the acceleration cycle. The orbit exists when the well-known *betatron condition* is satisfied. The confinement properties of the system for nonideal orbits are subsequently discussed.

The derivations demonstrate two properties of orbits: (1) particles injected on a circular orbit inside or outside the main orbit approach the main orbit during acceleration and (2) the amplitude of transverse oscillations decreases during the acceleration cycle. Section 11.3 addresses the first effect, motion of the instantaneous circle. Section 11.5 discusses damping of relativistic betatron

oscillations during acceleration. As an introduction, Section 11.4 reviews the properties of periodic particle motions under the influence of slowly changing forces. The laws governing reversible compressions, both for nonrelativistic and relativistic particles, are discussed. The results are applicable to a wide variety of accelerators and particle confinement devices. Section 11.6 covers injection and extraction of electrons from the machine.

Section 11.7 surveys betatron magnet circuits, proceeding from simple low-energy devices to high-energy accelerators with optimal use of the core. The betatron magnet provides fields for particle acceleration, beam bending, and particle confinement. The magnet must be carefully designed in order to fulfill these functions simultaneously. Ferromagnetic materials are an integral

part of all betatrons except the smallest laboratory devices. Thus, the available flux change is limited by the saturation properties of iron. Within these limits, the magnet circuit is designed to achieve the highest beam kinetic energy for a given stored modulator energy.

Even with good magnet design, existing betatrons are inefficient. Conventional betatrons rely on gradients of the bending field for focusing and utilize low-energy electron injection. The self-electric field of the beam limits the amount of charge that can be contained during the low-energy phase of the acceleration cycle. Usually, the beam current is much smaller than the driving circuit leakage current. Consequently, energy losses from hysteresis and eddy currents in the core are much larger than the net beam energy. Efficiency is increased by high beam current. Some strategies for high-current transport are discussed in Section 11.6. The two most promising options are (1) addition of supplemental focusing that is effective at low energy and (2) high-energy electron injection using a linear induction accelerator as a preaccelerator. In principle, betatrons can produce beam powers comparable to linear induction accelerators with a considerable reduction in isolation core mass.

11.1 PRINCIPLES OF THE BETATRON

Figure 11.1 illustrates the basic betatron geometry. A toroidal vacuum chamber encircles the core of a large magnet. The magnetic field is produced by pulsed coils; the magnetic flux inside the radius of the vacuum chamber changes with time. Increasing flux generates an azimuthal

Betatron

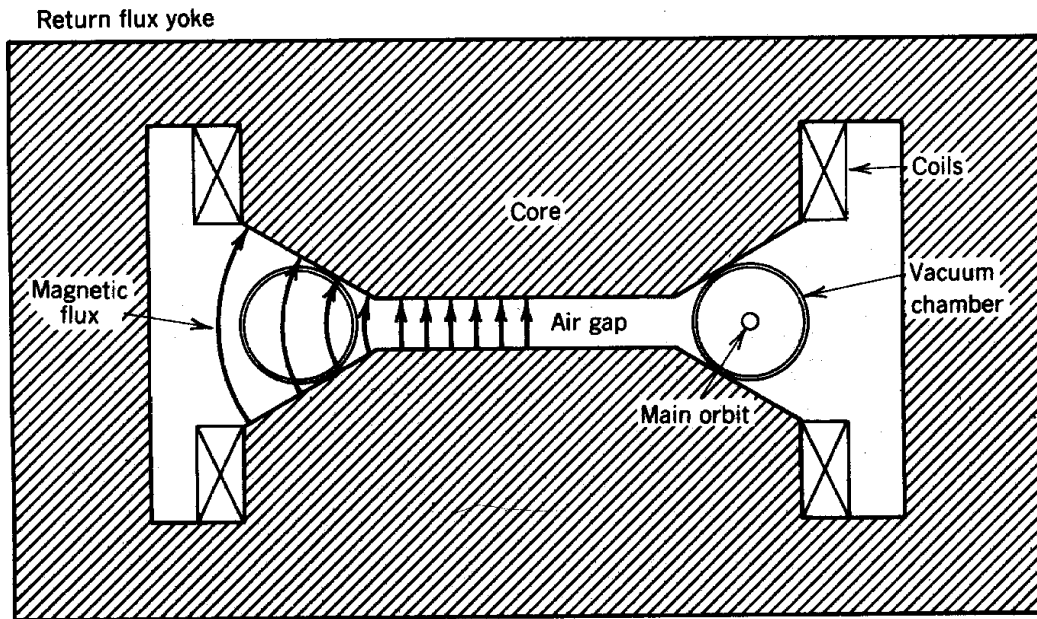


Figure 11.1 Schematic diagram of betatron with air gap.

electric field which accelerates electrons in the chamber.

In the absence of an air gap, there is little magnetic flux outside the core. An air gap is included to divert some of the magnetic flux into the vacuum chamber. By the proper choice of gap width, the vertical magnetic field can be adjusted to confine electrons to a circular orbit in the vacuum chamber. As shown in Figure 11.1, the confining field lines are curved. The resultant field has a positive field index. As we found in Section 7.3, the field can focus in both the horizontal and vertical directions.

In summary, the simple betatron of Figure 11.1 has the following elements:

1. A pulsed magnet circuit to accelerate electrons by inductive fields.
2. An air gap to force magnetic field into the beam transport region; electrons follow circular orbits in the bending field.
3. Shaped magnetic fields for beam focusing.

At first glance, the betatron appears quite different from the linear induction accelerator. Nonetheless, we can show that the power circuits of the two devices are similar. To begin, consider the induction accelerator illustrated in Figure 11.2a. The geometry is often called a *recirculating induction linac*. The transport tube is bent so that the beam passes through the same cavity a number of times. This allows higher beam kinetic energy for a given volt-second

Betatrons

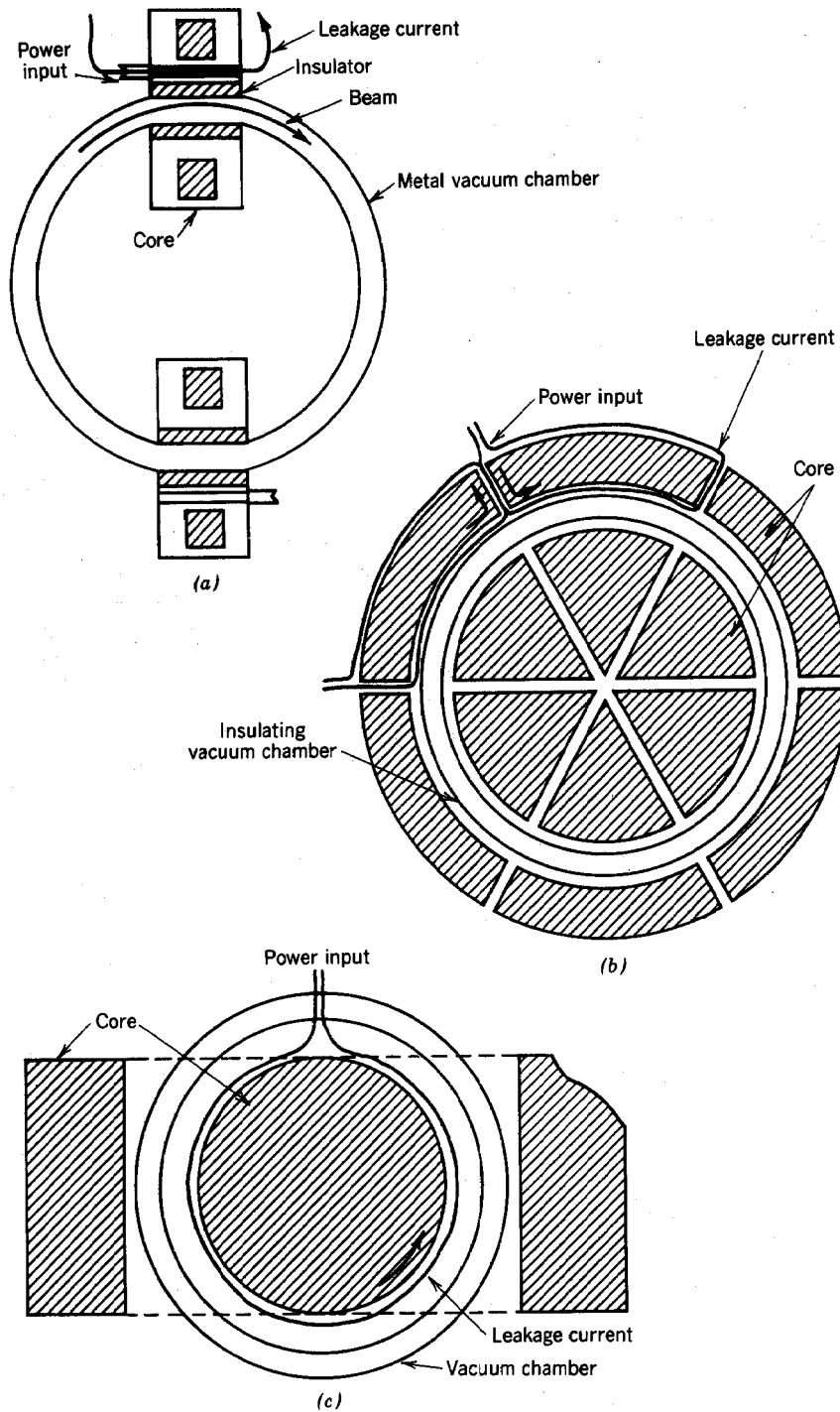


Figure 11.2 Equivalence between betatrons and linear induction accelerators. (a) Recirculating induction linac with two acceleration cavities. (b) Recirculating induction linac with isolation cores that fill the available area inside beam orbit. (c) Betatron with single core and single power feed point.

Betatrons

product of the isolation cores. The transport tubes are made of metal; each cavity has separate vacuum insulators and high-voltage feeds. There are supplemental magnetic or electric forces to bend the orbits and keep particles confined in the tube.

To begin, we calculate the maximum electron kinetic energy possible in a recirculating induction linac with the following assumptions:

1. The beam tube has circumference $2\pi R$.
2. There are N cavities around the circumference; each cavity has an isolation core with cross-sectional area A_c .
3. The accelerating waveform in a cavity is a square pulse with voltage V_o and the pulselength t_p .
4. Over most of the acceleration cycle, electrons travel near the velocity of light.

During the acceleration cycle, the electrons make $ct_p/2\pi R$ revolutions and travel through $Nct_p/2\pi R$ cavities. The final kinetic energy is therefore

$$E_b = V_o t_p Nc/2\pi R \text{ (eV)}. \quad (11.1)$$

Equation (11.1) can be rewritten by expressing the volt-second product in terms of the core properties [Eq. (10.1)]:

$$E_b \leq 2B_s NA_c c/2\pi R. \quad (11.2)$$

For a given circumference, the highest energy is attained with the tightest packing of isolation cores around the beam tube. The packing limit is reached when the cores fill the area inside the beam, $NA_c = \pi R^2$. Making this substitution, we find that

$$E_b \leq 2B_s Rc/2. \quad (11.3)$$

An optimized recirculating induction accelerator with pie-shaped cores is shown in Figure 11.2b. In the figure, much of the structure has been removed and the vacuum insulators have been extended to produce a single nonconducting toroidal vacuum chamber. The final step is to recognize that the radial currents of the individual power feeds cancel out; we can replace the multiple voltage feeds with a single line that encircles the core. Power is supplied from a single-pulse modulator. The resulting geometry, the power circuit of the betatron, is shown in Figure 11.2c.

In summary, the main differences between the betatron and the linear induction accelerator are as follows:

1. The betatron has one pulse modulator; the induction accelerator has many.

Betatrons

2. The beam in an induction accelerator makes a single pass through the machine. The equivalent circuit is a transformer with a single-turn secondary and multiple parallel primary windings. In the betatron, the beam makes many revolutions around the core. The circuit representing this machine is a single primary with a multi-turn secondary.
3. Because of recirculation, average gradient is not a concern in the betatron. Therefore, low accelerating voltages and relatively long pulselengths (matched to the available volt-second product of the core) are used. The circuit of Figure 11.2c requires a slow voltage pulse because it has significantly higher inductance than the driving circuits of Figure 11.2b.
4. Shaping of the voltage pulse shape is not important in the betatron. The beam is distributed uniformly around the transport tube; there is no need for longitudinal confinement. The betatron magnet is usually driven by a bipolar, harmonic voltage waveform that cycles the core between $-B_s$ and $+B_s$.

The slow acceleration cycle and small circuit voltage allow a number of options for construction of the transport tube. The tube may be composed of metal interrupted azimuthally by one or more insulating rings. It is also possible to use a metal chamber constructed of thin stainless steel; the wall resistance must be high enough to keep inductively driven return currents small.

Equation 11.3 is also applicable to the betatron. As an example of kinetic energy limits, take $R = 1$ m and $B_s = 1.5$ T. The maximum kinetic energy is less than 450 MeV. Equation (11.3) has an important implication for the scaling of betatron output energy. The beam energy increases linearly with the radius of the central core, while the volume of core and flux return yoke increase as R^3 . Cost escalates rapidly with energy; this is one of the main reasons why betatrons are limited to moderate beam energy.

As a final topic, we shall consider why betatrons have little potential for ion acceleration. In the discussion, ion dynamics is treated nonrelativistically. Assume an ion of mass m_i is contained in a betatron with radius R ; the emf around the core is V_0 . The energy ions gain in a time interval Δt is eV_0 multiplied by the number of revolutions, or

$$dE_b' = (eV_0/2\pi R) \sqrt{2E_b'/m_i} \Delta t. \quad (11.4)$$

Equation (11.4) can be rearranged to give

$$dE_b'/E_b'^{1/2} = (V_0/2\pi R) \sqrt{2e^2/m_i} \Delta t. \quad (11.5)$$

Integrating Eq. (11.5) (with the assumption that the final ion energy E_b is much larger than the injection energy), we find that

Betatrons

$$\sqrt{E_b} \leq \sqrt{e/2m_i} (V_0 t_p / 2\pi R) \text{ (eV)}. \quad (11.6)$$

Substituting for the volt-second product and assuming a core area πR^2 , Eq. (11.6) can be rewritten

$$E_b \leq (2e/m_i) (B_s R/2)^2. \quad (11.7)$$

With the same magnet parameters as above ($R = 1 \text{ m}$, $B_s = 1.5 \text{ T}$), Eq. (11.7) implies that the maximum energy for deuterons is only 54 MeV. Comparing Eq. (11.7) to Eq. (11.3), we find that the ratio of maximum obtainable energies for ions compared to electrons is

$$E_b \text{ (ions)} / E_b \text{ (electrons)} = v_{if} / c, \quad (11.8)$$

where v_{if} is the final ion velocity. Equation (11.8) has a simple interpretation. During the same acceleration cycle, the nonrelativistic ions make fewer revolutions around the core than electrons and gain a correspondingly smaller energy.

11.2 EQUILIBRIUM OF THE MAIN BETATRON ORBIT

The magnitude of the magnetic field at the orbit radius of electrons in a betatron is determined by the shape of the magnet poles. The equilibrium orbit has the following properties: (1) the orbit is circular with a radius equal to that of the major radius R of the vacuum chamber and (2) the orbit is centered in the symmetry plane of the field with no vertical oscillations. This trajectory is called the *main orbit*. We will consider other possible orbits in terms of perturbations about the main orbit.

The vertical field at R is designated $B_z(R)$. Equation (3.38) implies that $B_z(R)$ and R are related by

$$R = \gamma m_e v_\theta / e B_z(R) = p_\theta / e B_z(R). \quad (11.9)$$

The quantity p_θ is the total momentum of particles on the main orbit. The magnetic field varies with time. The azimuthal electric field acting on electrons is

$$\int \mathbf{E} \cdot d\mathbf{l} = d\Phi/dt = 2\pi R E_\theta, \quad (11.10)$$

Betatrons

where Φ is the magnetic flux enclosed within the particle orbit. Particle motion on the main orbit is described by the following equations:

$$\begin{aligned} v_r &= 0, & dp_r/dt &= 0, \\ v_z &= 0, & dp_z/dt &= 0, \\ dp_\theta/dt &= eE_\theta = (e/2\pi R) d\Phi/dt. \end{aligned} \tag{11.11}$$

Equation (11.11) is obtained from Eq. (3.34) by setting $v_r = 0$. We assume that R does not vary in time; consequently, Eq. (11.11) can be integrated directly to give

$$p_\theta = e [\Phi(t) - \Phi(0)]/2\pi R = (e/2\pi R) \Delta\Phi. \tag{11.12}$$

Combining Eqs. (11.9) and (11.12),

$$B_z(R) = \Delta\Phi/2\pi R^2. \tag{11.13}$$

Equation (11.13) is the well-known *betatron condition*. The betatron pole piece is designed so that vertical field at the average beam radius is equal to one-half the flux change in the core divided by the area inside the particle orbit. The betatron condition has a simple interpretation for the machine illustrated in Figure 11.1. Electrons are injected at low energy when the orbital field and the flux in the core are near zero. The bending field and accelerating field are produced by the same coils, so that they are always proportional if there is no local saturation of the core iron. The main orbit has radius R throughout the acceleration cycle if the vertical field at R is

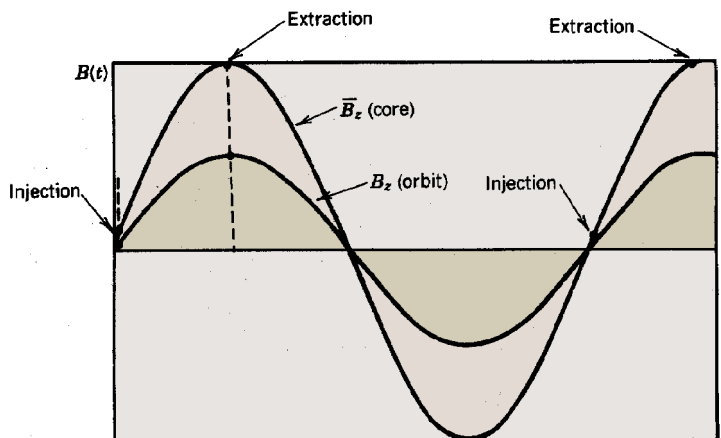


Figure 11.3 Acceleration cycle of air gap betatron; average magnetic field inside electron orbit and vertical magnetic field at main orbit as a function of time.

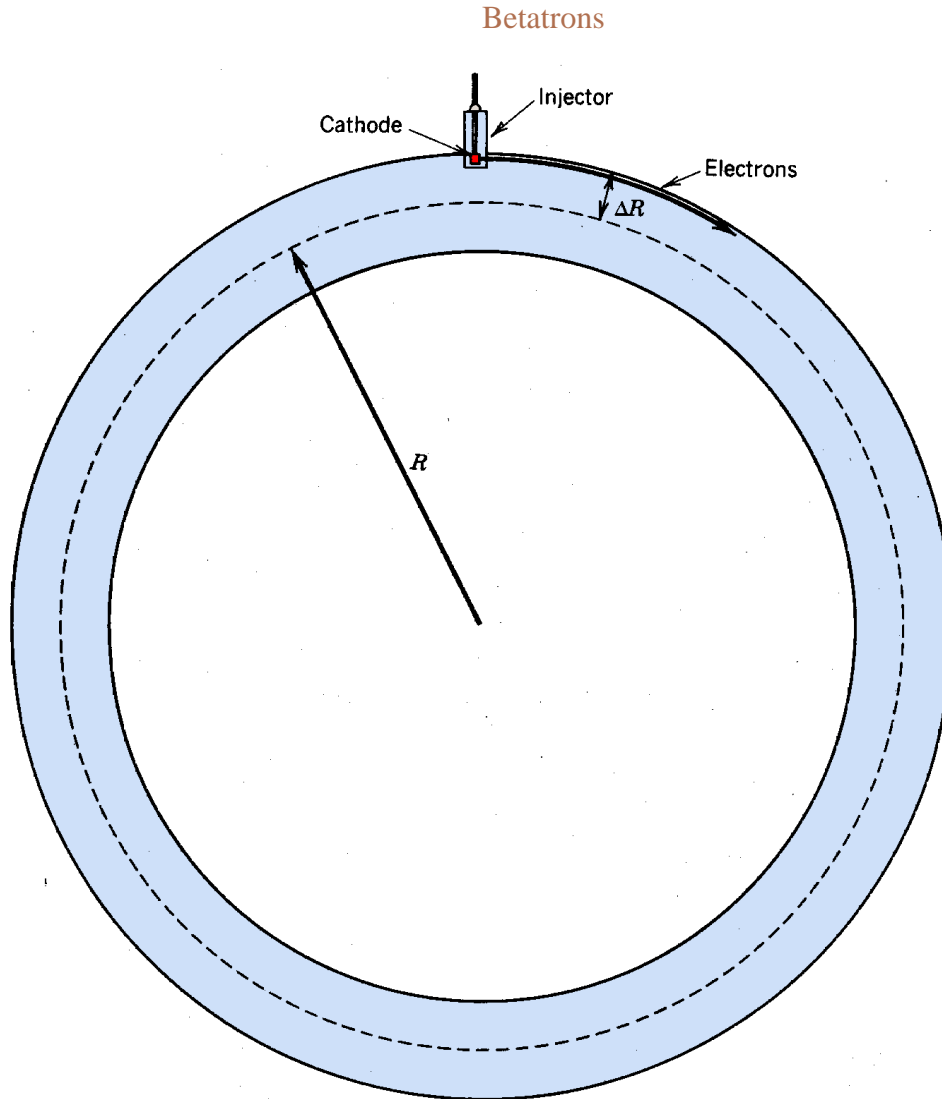


Figure 11.4 Injector geometry for low-current betatron.

equal to one-half the average field enclosed by the orbit. This condition holds both in the nonrelativistic and relativistic regimes. The acceleration cycle is illustrated in Figure 11.3.

11.3 MOTION OF THE INSTANTANEOUS CIRCLE

The standard electron injector of a betatron consists of a thermionic source at high dc voltage (20-120 kV) with extractor electrodes (Fig. 11.4). It is clear that such a device cannot extend to the main orbit. The injector is located at a radius inside or outside the main orbit and is displaced vertically from the symmetry plane. The extractor voltage is set so that the electrons have a circular orbit of radius $R + \Delta R$ in the magnetic field at injection. The betatron condition is not

Betatrons

satisfied on this orbit; therefore, the orbit radius changes during the acceleration cycle. We shall see that the orbit asymptotically approaches the main orbit as the electron energy increases. The circular orbit with slowly varying radius is referred to as the *instantaneous circle*.

Let p_0 be the momentum of a particle on the main orbit and p_1 be the momentum of a particle injected a distance ΔR from the main orbit on the instantaneous circle. At injection, the momenta and magnetic fields are related by

$$p_0(0) = eB_z(R)R, \quad (11.14)$$

$$p_1(0) = p_0(0) + \delta p(0) = eB_z(R+\Delta R)(R+\Delta R). \quad (11.15)$$

The time variation of flux enclosed within the instantaneous circle is

$$d\Phi_1/dt = 2\pi R^2 [dB_z(R)/dt] + \int_R^{R+\Delta R} 2\pi r dr [dB_z(r)/dt]. \quad (11.16)$$

Equation (11.13) has been used in the first term to express the magnetic flux in the region $0 < r < R$. Assume that field variations are small over the region near the main orbit so that $B_z(r) \cong B_z(R)$. To first order in Δr , Eq. (11.16) can be rewritten

$$d\Phi_1/dt \cong 2\pi R^2 [dB_z(R)/dt] + 2\pi R \Delta R (dB_z/dt) = 2\pi Rr [dB_z(R)/dt]. \quad (11.17)$$

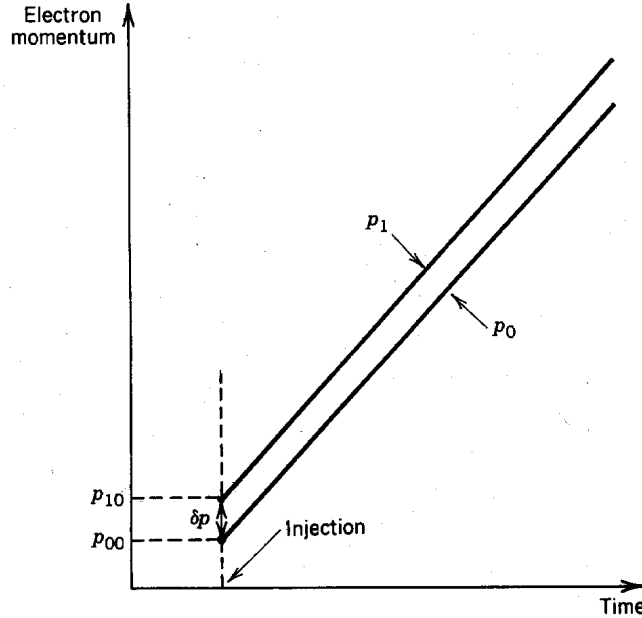


Figure 11.5 Time variation of momentum of electron on main orbit (p_0) and electron injected on instantaneous circle outside main orbit (p_1).

Betatrons

The equation of motion for an electron on the instantaneous circle is

$$dp_1/dt = (e/2\pi r) (d\Phi_1/dt) \cong eR [dB_z(R)/dt]. \quad (11.18)$$

We recognize that the expression on the right-hand side is equal to dp_o/dt [Eq. (11.14)].

The main conclusion is that particles on the instantaneous circle gain momentum at the same rate as particles on the main orbit, as illustrated in Figure 11.5. The ratio of the radius of the instantaneous circle to that of the main orbit is equal to the relative momentum difference, or

$$\delta p/p_o \cong \Delta R/R. \quad (11.19)$$

The radius difference is proportional, to $1/p_o$ because δp is constant by Eq. (11.18). Therefore, the instantaneous circle approaches the main orbit as the electron energy increases.

11.4 REVERSIBLE COMPRESSION OF TRANSVERSE PARTICLE ORBITS

As we saw in Section 7.3, the focusing strength of magnetic field gradients is proportional to the magnitude of the bending field. In order to describe the betatron, the derivations of particle transport in continuous focusing systems must be extended to include time-varying focusing forces. As an introduction, we will consider the general properties of periodic orbits when the confining force varies slowly compared to the period of particle oscillations. The approximation of slow field variation is justified for the betatron; the transverse oscillation period is typically 10-20 ns while the acceleration cycle is on the order of 1 ms. The results are applicable to many beam transport systems.

To begin, consider the nonrelativistic transverse motion of a particle under the action of a force with a linear spatial variation. The magnitude of the force may change with time. The equation of motion is

$$d^2x/dt^2 = - [F(t)/mx_o] x = -\omega(t)^2 x. \quad (11.20)$$

If the time scale for the force to change, ΔT , is long compared to $1/\omega$, then the solution of Eq. (11.20) looks like the graph of Figure 11.6. The relative change in ω over one period, $\Delta\omega$, is small:

$$\Delta\omega/\omega \ll 1. \quad (11.21)$$

Betatrons

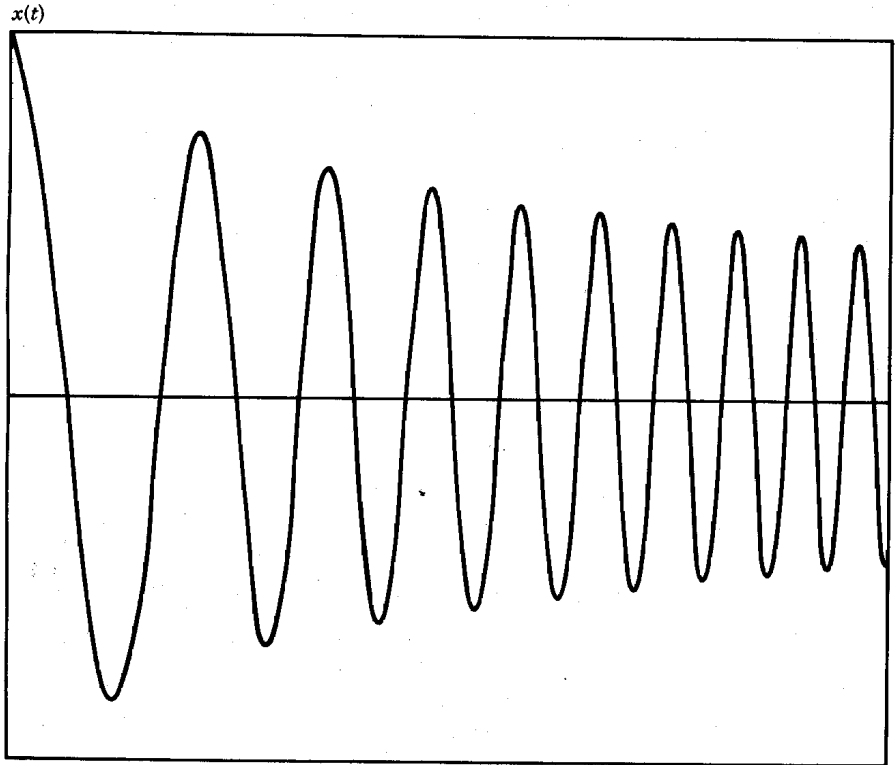


Figure 11.6 Time-dependent displacement of particle acted on by a focusing force that increases with time. Force varies linearly with x and increases a factor of 5 over time interval shown.

The condition of Eq. (11.21) can be rewritten in two alternate forms:

$$\frac{(d\omega/dt) (1/\omega)}{\omega} = \frac{d\omega/dt}{\omega^2} \ll 1, \quad (11.12)$$

$$\frac{1}{\omega \Delta T} \ll 1. \quad (11.23)$$

Equations (11.21)-(11.23) give the condition for a *reversible compression* (or *reversible expansion*). The meaning of reversible will be evident when we consider properties of the particle orbits.

Following Figure 11.6, an approximate solution to Eq. (11.20) should be oscillatory with a slow variation of amplitude. We assume a form

$$x(t) = A(t) \sin[\Phi(t)]. \quad (11.24)$$

Betatrons

The quantities $A(t)$ and $\Phi(t)$ are determined by substituting Eq. (11.24) into Eq. (11.20) and dropping terms of order $(1/\omega\Delta T)^2$ or higher.

Calculating the derivatives and substituting,

$$x = (d^2A/dt^2)\sin\Phi + 2(dA/dt)(d\Phi/dt)\cos\Phi - A\sin\Phi(d\Phi/dt)^2 + A(d^2\Phi/dt^2)\cos\Phi = -\omega^2\sin\Phi.$$

The solution must hold at all values of Φ . Therefore, the $\sin\Phi$ and $\cos\Phi$ terms must be individually equal, or

$$(d^2A/dt^2) - A (d\Phi/dt)^2 = -\omega^2 A, \quad (11.25)$$

$$2 (dA/dt) (d\Phi/dt) + A (d^2\Phi/dt^2) = 0. \quad (11.26)$$

The first term in Eq. (11.25) is of order $A/\Delta T^2$. This term is less than the expression on the right-hand side by a factor $(1/\omega\Delta T)^2$, so it can be neglected. Equation (11.25) becomes $d\Phi/dt = \omega$; therefore,

$$\Phi = \int \omega dt + \Phi_o. \quad (11.27)$$

Substituting this expression in Eq. (11.26) gives

$$2 (dA/dt)/A = - (d^2\Phi/dt^2)/(d\Phi/dt) \cong - (d\omega/dt)/\omega. \quad (11.28)$$

Integrating both sides of Eq. (11.28),

$$\ln(\omega) = -2 \ln(A) + \text{const.}$$

or

$$\omega A^2 = \text{const.} \quad (11.29)$$

The approximate solution of Eq. (11.20) is

$$x(t) \cong A_o \sqrt{\omega_o/\omega} \sin\left(\int \omega dt + \Phi_o\right). \quad (11.30)$$

Taking the derivative of Eq. (11.30), the particle velocity is

Betatrons

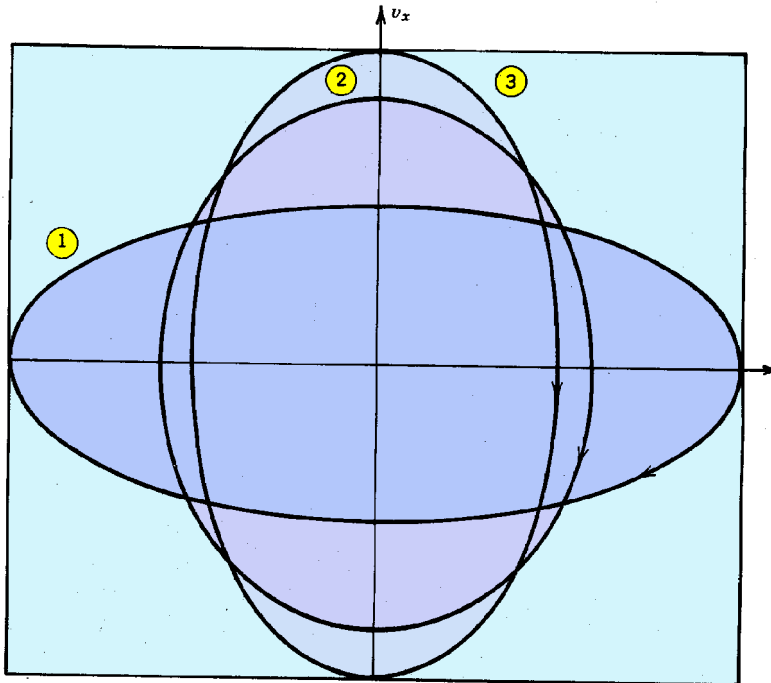


Figure 11.7 Variation of particle phase space orbits during reversible compression. (1) Initial orbit influenced by force that varies linearly with x . (2) Magnitude of force increased by a factor of 8. (3) Magnitude of force increased by a factor of 16.

$$\begin{aligned}
 x(t) &\cong A_o \sqrt{\omega_o/\omega} \left[\cos\left(\int \omega dt + \Phi_o \right) - ((d\omega/dt)/2\omega^2) \sin\left(\int \omega dt + \Phi_o \right) \right] \\
 &\cong A_o \sqrt{\omega_o/\omega} \cos\left(\int \omega dt + \Phi_o \right).
 \end{aligned}
 \tag{11.31}$$

Hving solved the problem mathematically, let us consider the physical implications of the results.

1. At a particular time, the particle orbits approximate harmonic orbits with an angular frequency ω determined by the magnitude of the force. The amplitude and angular frequency of the oscillations changes slowly with time.
2. As the force increases, the amplitude of particle oscillations decreases, $x_{\max} \sim 1/\sqrt{\omega}$. This process is called compression of the orbit.
3. The particle velocity is approximately 90° out of phase with the displacement.
4. The magnitudes of the velocity and displacement are related by

Betatrons

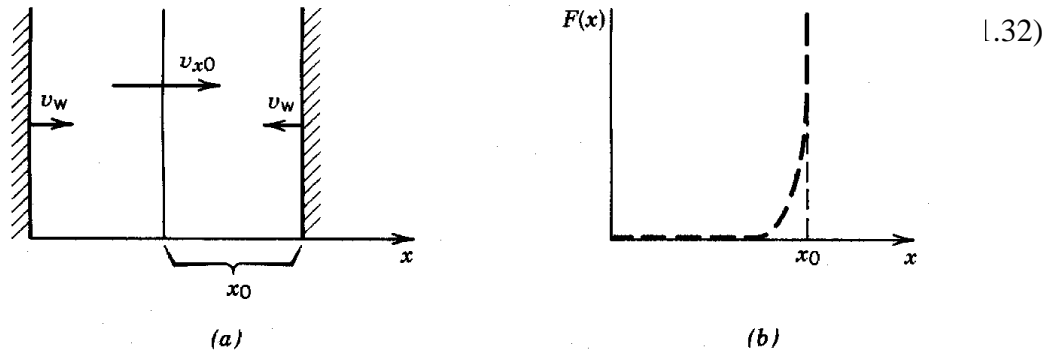


Figure 11.8 Particle confinement in a square well. (a) Geometry and coordinates, particle reflected elastically between two walls. (b) Variation of force with x .

5. The product of the displacement and velocity is conserved in a reversible process, or

$$x_{\max} v_{x,\max} \cong \text{const.} \quad (11.33)$$

Figure 11.7 gives a graphical interpretation of the above conclusions. Particle orbits are plotted in phase space with x and v_x as axes. Inspection of Eqs. (11.30) and (11.31) shows that particle

orbits acted on by a linear force are ellipses in phase space. Orbits are plotted in Figure 11.7 for a slow increase in focusing force (reversible compression). Although the oscillation amplitude changes, the net phase space area included within the orbit is constant. If the force slowly returns to its initial value, the particle orbit is restored to its original parameters; hence, the term reversible.

The properties of reversible compressions are not limited to linear forces but hold for confinement forces with any spatial variation. Consider, for instance, a particle contained by the square-well potential illustrated in Figure 11.8. The force is infinite at $x = x_0$ and $x = -x_0$. The particle has constant velocity v_{x0} except at the reflection points. The walls move inward or outward slowly compared to the time scale $x_0(t)/v_{x0}(t)$. In other words, the constant wall velocity v_w is small compared to $v_{x0}(t)$ at all times.

Particles reflect from the wall elastically. Conservation of momentum implies that the magnitude of v_{x0} is constant if the wall is stationary. If the wall moves inward at velocity v_w , the particle velocity after a collision is increased by an amount

$$\Delta v_{x0} = 2v_w. \quad (11.34)$$

In a time interval Δt , a particle collides with the walls $v_{x0}(t)\Delta t/2x_0(t)$ times. Averaging over many collisions, we can write the following differential equation:

Betatrons

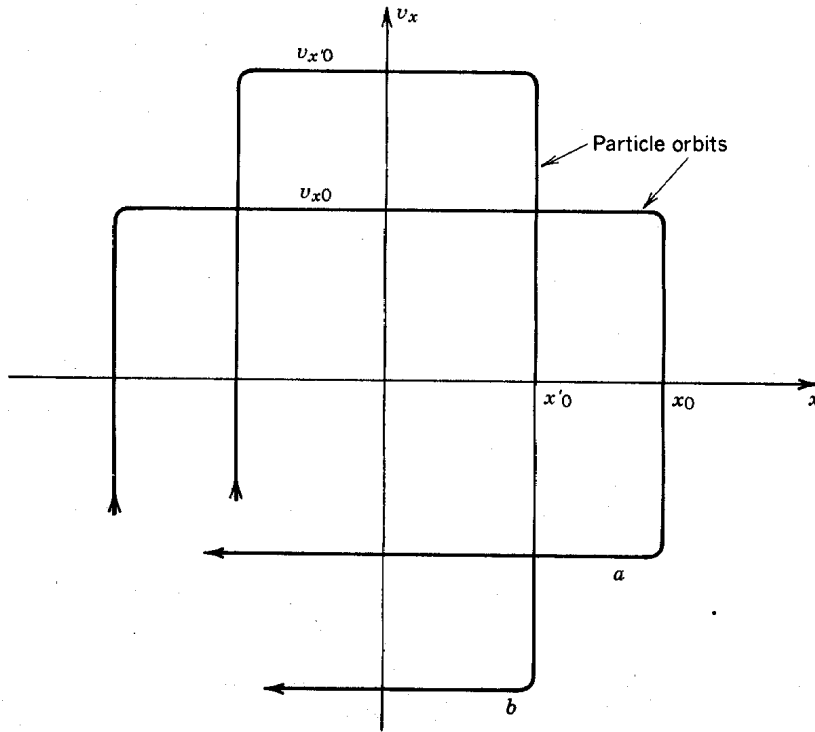


Figure 11.9 Phase space orbits of particles confined between two reflecting walls that move inward slowly. (a) Initial orbit. (b) Orbit with distance between walls decreased by a factor of 2.

$$dv_{x'o}/dt \cong 2v_w v_{x'o}(t)/2x_o(t). \quad (11.35)$$

The equation of the wall position is $x_o(t) = x_o(0) - v_x(t)t$, or

$$dx_o = -v_w dt. \quad (11.36)$$

Substituting into Eq. (11.35), we find $dv_{x'o}/v_{x'o} = -dx_o/x_o$, or

$$x_o(t) v_{x'o}(t) \cong \text{const.} \quad (11.37)$$

This is the same result that we found for the harmonic potential. Similarly, defining the periodic frequency $\omega = v_{x'o}(t)/x_o(t)$, Eq. (11.37) implies that

$$x_o \sim 1/\sqrt{\omega},$$

Betatrons

or

$$x_o^2 \omega = \text{const.} \quad (11.38)$$

as before. A phase space plot of particle orbits in a highly nonlinear focusing system during a reversible compression is given in Figure 11.9.

11.5 BETATRON OSCILLATIONS

Reviewing the conclusions of Section 7.3, particles in a gradient magnetic field perform harmonic oscillations about the main orbit in the radial and vertical directions. The frequencies of oscillation are

$$\omega_r = \omega_g \sqrt{1-n}, \quad (11.39)$$

$$\omega_z = \omega_g \sqrt{n}, \quad (11.40)$$

where n is the field index and $\omega_g = eB_z(R)/\gamma m_e$. In the betatron, the magnitude of the magnetic field increases (ω_g is a function of time) while the relative shape remains constant (n is constant). The focusing force increases; therefore, the amplitude of oscillations in the radial and vertical directions decreases and particles move closer to the main orbit. This process is often called damping of betatron oscillations, although this is a misnomer. The process is reversible and no dissipation is involved.

The mathematical description of betatron oscillations is similar to that of Section 11.4 except that the variation of electron mass with energy must be taken into account for relativistically correct results. We shall consider motion in the vertical direction; the derivation for radial motion is a straightforward extension. With the assumption that $v_z \ll v_0$, the transverse approximation (Section 2.10) can be applied. This means that vertical motions do not influence the value of γ .

The vertical equation of motion for a linear force can be written

$$dp_z(t)/dt = d[m(t)v_z(t)]/dt = -m(t) \omega_z(t)^2 z. \quad (11.41)$$

Expanding the time derivative, Eq. (11.41) becomes

$$(d^2z/dt) + (dm/dt)(dz/dt)/m + \omega_z^2 z = 0. \quad (11.42)$$

Again, we seek a solution of the form

Betatrons

$$z = A(t) \sin\Phi_z(t). \quad (11.43)$$

Substituting in Eq. 11.42,

$$\begin{aligned} (\omega_z^2 - \Phi_z^2) A \sin\Phi_z + [A(d^2\Phi_z/dt^2) + 2(dA/dt)(d\Phi_z/dt) + A(dm/dt)(d\Phi_z/dt)/m] \cos\Phi_z \\ + [(d^2A/dt^2) + (dA/dt)(dm/dt)/m] \sin\Phi_z = 0. \end{aligned} \quad (11.44)$$

We can show by dimensional arguments that the third term of Eq. (11.44) is smaller than the first term by a factor of $(1/\omega\Delta T)^2$, where ΔT is the time scale of the acceleration cycle. Therefore, to first order, the first term is approximately equal to zero:

$$\omega_z^2 = (d\Phi_z/dt)^2. \quad (11.45)$$

Equation (11.45) gives the same result as the nonrelativistic derivation [Eq. (11.27)]:

$$\Phi_z = \int \omega_z dt + \Phi_0. \quad (11.46)$$

Setting the second term equal to zero gives

$$A (d^2\Phi_z/dt^2) + 2 (dA/dt) (d\Phi_z/dt) + A [(dm/dt)/m] \Phi_z = 0. \quad (11.47)$$

We can show that Eq. (11.47) is equivalent to

$$d(A^2 m \omega_z)/dt = 0,$$

or

$$A^2 m \omega_z = \text{const.} \quad (11.48)$$

There are some interesting implications associated with the above derivation. As before, the vertical displacements and velocity are 90° out of phase with magnitudes related by

$$v_{z,\max} \cong z_{\max} \omega_z = A \omega_z. \quad (11.49)$$

Betatrons

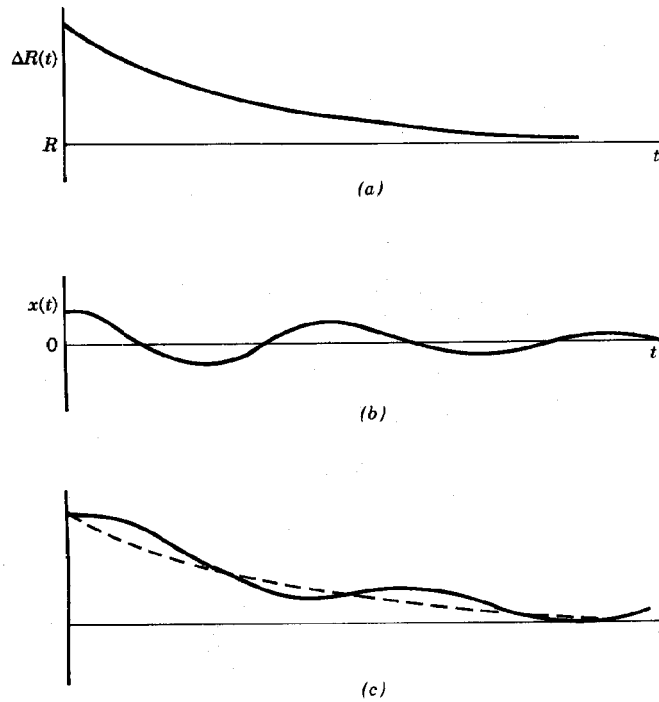


Figure 11.10 Schematic view of orbit of electron injected into low-current betatron. (a) Motion of instantaneous circle toward main orbit. (b) Reversibly compressed betatron oscillations. (c) Composite orbit.

The conservation law for a relativistic reversible compression is

$$m v_{z,\max} z_{\max} = z_{\max} P_{z,\max} = \text{const.} \quad (11.50)$$

For relativistic particles, the area circumscribed by an orbit is constant if it is plotted in phase space axes of displacement and momentum rather than displacement and velocity.

11.6 ELECTRON INJECTION AND EXTRACTION

Particle injection into linear accelerators is not difficult. In contrast, injection is a significant problem for circular accelerators, particularly those with constant beam radius such as the betatron. This is one of the reasons why high current electron beams have not yet been accelerated in betatrons. The conventional betatron electron source consists of a thermionic cathode located in the vacuum chamber (Fig. 11.4) capable of emitting 1-2 A current. The cathode is biased to high negative potential and electrons are extracted and focused by shaped electrodes. The emerging beam has a large spread in particle direction. The source is pulsed on for a few microseconds at the time when electrons will travel on an instantaneous circle orbit in

Betatron

the rising bending magnetic field.

Following injection, the combined effects of inward motion of the instantaneous circle and damping of betatron oscillations carries electrons away from the injector so that some are trapped. The process is illustrated in Figure 11.10. Without such effects, the electrons would eventually strike the back of the injector. The fraction of electrons trapped is increased if the injector is

displaced vertically from the main orbit. Because of the vertical oscillations, particles may travel many revolutions before striking the injector, even in the absence of radial motion.

As an example, consider a 300-MeV betatron with main orbit radius of 1 m operating at 180 Hz. The rate of energy gain is about 7 keV/turn. If the injection energy is 100 keV and the initial instantaneous circle has radius 1.05 m, then Eq. (11.19) implies that the orbit moves radially inward a distance 0.24 cm in a single turn. If vertical oscillations allow the particles 5-10 turns,

this radial motion is sufficient to trap a substantial number of electrons.

The main limit on trapping in a high-energy betatron appears to result from beam space charge effects. Focusing is weak at injection because of the low applied magnetic field. In the example above, the injection field is only 10^{-3} T. Estimating the space charge force and specifying a balance with the vertical focusing force leads to a predicted equilibrium current of less than 1 A for a

beam with 4 cm vertical extent. This figure is consistent with the maximum current observed in betatrons. The dominant role of space charge in limiting injection current is consistent with the fact the trapped current increases significantly with increased injector voltage. The injection efficiency for high-energy betatrons with an internal, electrostatic injector is typically only a few percent.

Trapping mechanisms are not as easily explained in small, low-energy betatrons. In a machine with output energy of 20 MeV, motion of the instantaneous circle is predicted to be on the order of only 2×10^{-3} cm. Nonetheless, the trapped current is observed to be much higher than that predicted from single-particle orbit dynamics combined with the probability of missing the injector. The most widely accepted explanation is that collective particle effects are responsible for the enhanced trapping. There is a substantial inductance associated with the changes of beam

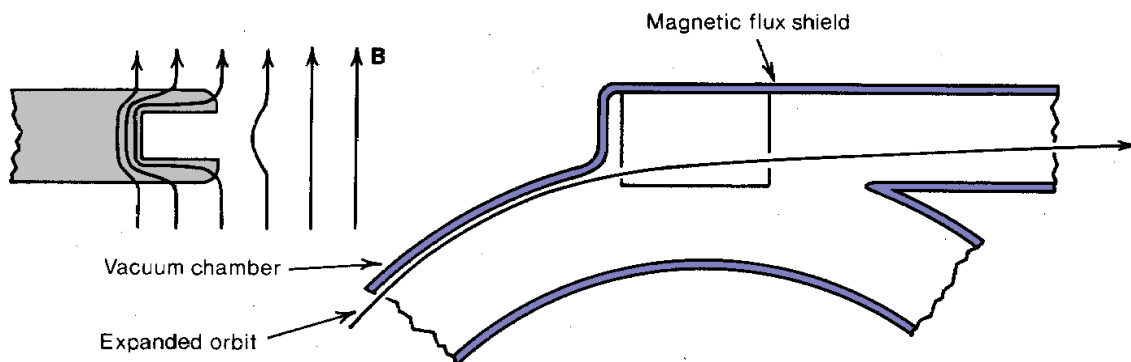


Figure 11.11 Extraction of low-current electron beam from betatron.

Betatron

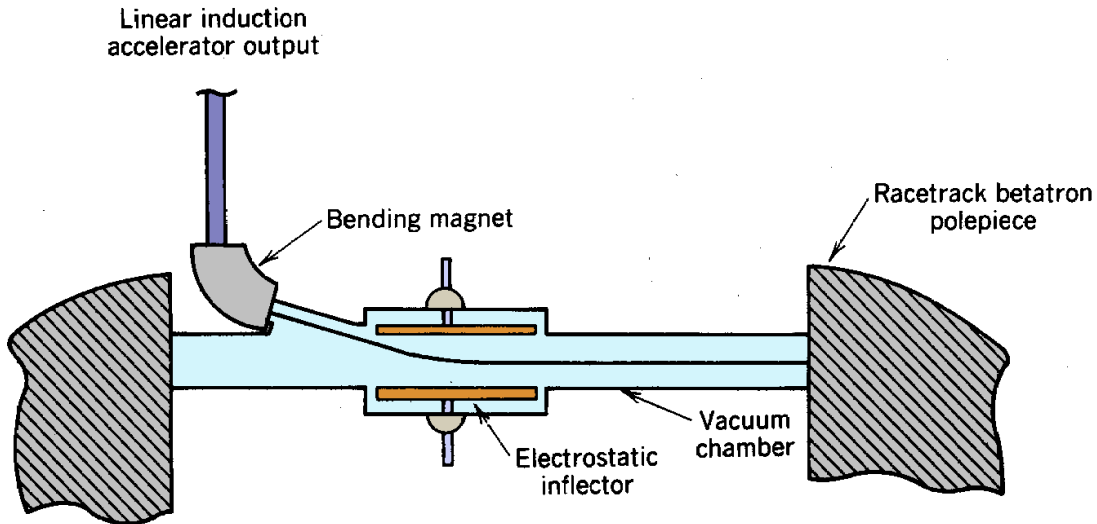


Figure 11.12 Injection of high-current electron beam from linear induction accelerator into racetrack betatron.

current around the ferromagnetic core. The increasing beam current during the injection pulses induces a back emf that is larger than the accelerating emf of the core. The inductive electric field decelerates electrons. The effect is almost independent of radius, so that particle orbits shrink toward the main orbit much more rapidly than predicted by the arguments of Section 11.3. This explanation is supported by the fact that trapping in low-energy betatrons is improved considerably when orbit contraction coils are incorporated in the machine. These rapidly pulsed coils enhance the self-field effects by inducing a back emf.

Extraction of electron beams from betatrons is accomplished with a magnetic peeler, illustrated in Figure 11.11. This device is a magnetic field shunt located on an azimuth outside the radius where $n = 1$. It cannot be located too close to the main orbit because the associated magnetic field perturbation would cause particle loss during the low-energy phase of the acceleration cycle. If particles are forced past the $n = 1$ radius, radial focusing is lost and they spiral outward into the peeler. There are a number of options for inducing radial motion of the betatron beam. One possibility is an orbit expander coil. The expander coil is activated at the peak of the electron energy. It subtracts from the bending field in the beam chamber, causing the beam radius to expand. Another method of moving electrons out in radius is to induce betatron oscillations by resonant fields. Electric or magnetic fields oscillating at $\sqrt{1-n} \omega_g$ are generated by coils or plates at particular azimuthal positions. If the growth of betatron oscillations is rapid, the beam spills out at a specific azimuth.

The maximum current that can be contained in a betatron is determined by a balance between the mutual repulsion between electrons and the focusing forces. In terms of space-charge equilibrium, the gradient focusing strength in a betatron at peak field (~ 1 T) is sufficient to contain a high-energy (~ 300 MeV) electron beam with current in excess of 10 kA. A high-energy electron beam is stiff and largely confined by its own magnetic fields; therefore, an extension of conventional betatron extraction techniques would be sufficient to extract the beam from the machine. Containing the beam during the low-energy portion of the acceleration phase

Betatrons

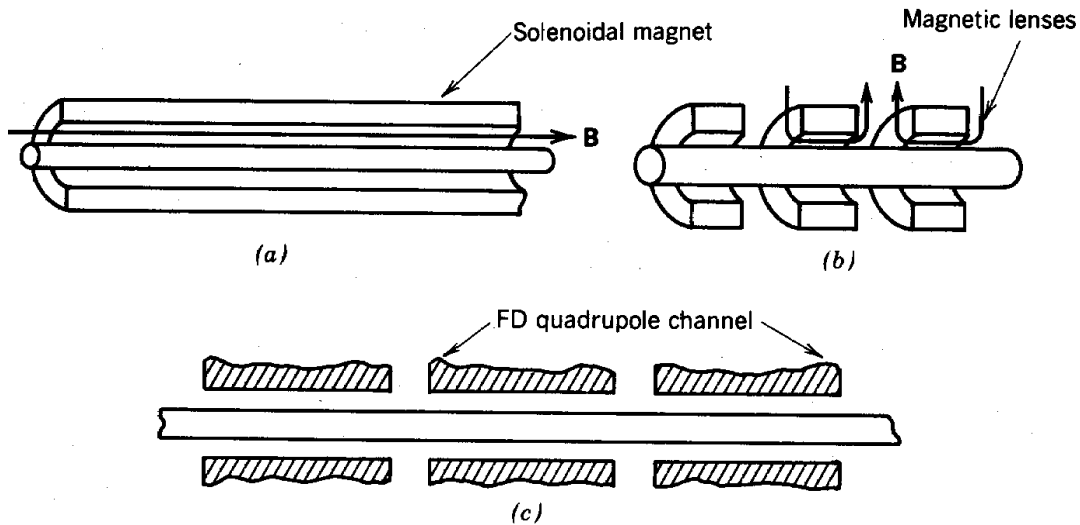


Figure 11.13 Methods to supplement focusing of low-energy electrons in betatron. (a) Magnet winding around vacuum chamber to produce uniform toroidal magnetic field. (b) Periodic array of magnetic lenses (with alternating field polarity) displaced around vacuum torus. (c) FD (or FODO) quadrupole lens array.

is the major impediment to a high-current, high-efficiency betatrons. Two methods appear feasible to improve the operation of betatrons: (1) high-energy injection and (2) addition of supplemental focusing devices.

In the first method, illustrated in Figure 11.12, a high-current, high-energy beam from a linear induction accelerator is injected in a single turn into the betatron. To facilitate injection, the betatron could be constructed in a racetrack configuration. The circular machine is split into two parts connected by straight sections. Injection and extraction are performed in the straight sections, which are free of bending fields. The betatron performs the final portion of the acceleration cycle (for example, from 100 to 300 MeV). The current limit in the betatron is high for two reasons: (1) the bending field and its gradients are large and (2) the self-magnetic field force of the relativistic beam almost balances the self-electric field repulsion so that space charge effects are of reduced importance. The beam is directed along the main orbit by a pulsed electrostatic inflector. The radial inflector field is activated only during a single transit of the beam around the accelerator; otherwise, it would deflect the trapped beam onto an exit orbit similar to the entrance orbit. The combination of induction linear accelerator and betatron is a good symbiosis for high-flux electron beams. The induction accelerator, with its strong solenoidal focusing magnets, solves the problem of injection and low-energy transport. The betatron provides the bulk of the particle acceleration. The combined accelerator would have a size and core volume much smaller than that of a 300-MeV linear induction accelerator.

A second approach to high-flux betatrons is to supplement gradient focusing with axi-centered focusing lenses arrayed around the toroidal vacuum chamber. Some options, illustrated in Figure 11.13, include (1) a bent solenoidal field (toroidal field), (2) discrete solenoidal magnetic lenses with reversing applied field direction, and (3) an array of magnetic quadrupole lenses in an

Betatrons

FD configuration. The study of alternate focusing methods in betatrons is an active area of research. There are some difficult technological problems to be solved. For instance, injection into a betatron with a strong toroidal field is considerably more difficult than injection into a standard geometry, even at low current. The main problem in any strong focusing betatron is the fact that

the beam must pass through the $\nu = 1$ condition (see Section 7.2). When the low-energy beam is injected, the strong space charge forces require strong supplementary focusing. Strong focusing implies that the betatron wavelength is less than the circumference of the machine; thus, $\nu > 1$ in both the radial and vertical directions. At the end of the acceleration cycle, gradient field focusing dominates. The orbits resemble those in a conventional betatron with $\nu < 1$. Passage through the resonance condition could be avoided by increasing the supplementary focusing fields with the bending fields and keeping $\nu > 1$. This is not technologically practical since the focusing system would require high energy input. Passage through the $\nu = 1$ condition may result in complete loss of the beam. There is a possibility that the severity of resonance instabilities could be reduced by a nonlinear focusing system, a fast acceleration cycle, or tuned electrostatic lenses that sweep the focusing system rapidly through the resonance condition.

11.7 BETATRON MAGNETS AND ACCELERATION CYCLES

The kinetic energy limit of betatrons is tied closely to the saturation properties of iron. Although air core betatrons have been operated successfully, they are impractical except for small research devices because of the large circulating energy and power losses involved. The volume of magnetic field outside the iron core should be minimized for the highest accelerator efficiency and lowest cost. With these factors in mind, we will review some of the types of betatron magnets that have been developed. The order will be roughly historical, proceeding from the simplest circuits at low energy to the highest energy attained.

An early betatron for electrons at 20 MeV is illustrated in Figure 11.1. The acceleration cycle is illustrated in Figure 11.3. The core flux and bending field are part of the same magnetic circuit; therefore, they are proportional to one another. A betatron driving circuit is illustrated in Figure 11.14. The inductance represents the betatron core and windings; a resistor has been included

to represent energy loss through winding resistivity, hysteresis, and eddy currents. The beam load is also indicated; at current typical of conventional betatrons, the impedance of the beam load is high. The beam current is much smaller than the leakage current. In order to keep the power consumed by the betatron at a reasonable level, the core inductor is often combined with a capacitor bank to form a resonant circuit. The leakage current is supported as reactive current in the resonant circuit; a fraction of the energy of the underdamped LC circuit is lost on each cycle to resistive losses and beam acceleration. The stored energy of the capacitor bank is topped up on each cycle by a driving circuit with high-power vacuum tubes.

The components of the resonant circuit fulfill the following conditions:

Betatrons

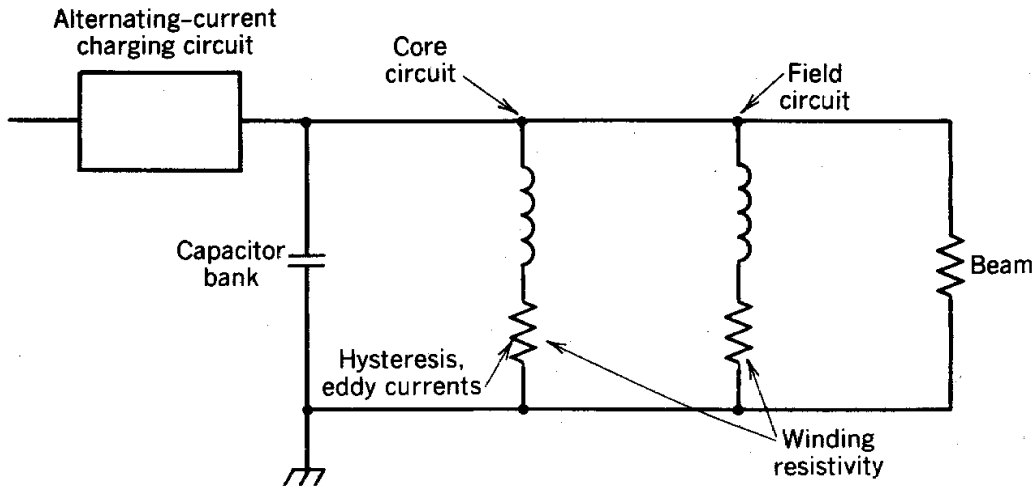


Figure 11.14 Alternating-current power circuit for a low-current betatron operated without core saturation.

1. The circuit has the desired resonant frequency, or

$$f = 2\pi / \sqrt{LC}.$$

Typically, betatrons operate at 180 Hz.

2. The stored energy in the capacitor bank, $\frac{1}{2}CV_0^2$, equals the total magnetic field energy at the peak of the acceleration cycle,

$$U_m = \int dx^3 (B^2/2\mu).$$

3. The ampere turns in the coil box are sufficient to produce the field in the air gap.

The above conditions can be combined to determine the capacitor bank voltage and number of turns in the coil box given the operating parameters of the betatron.

The betatron of Figure 11.1 has a major drawback for application to high-energy beams. Most of the energy in the drive circuit is utilized to produce magnetic flux in the central air gap. This translates into a large capacitor bank to store energy and increased resistive losses because of the high NI product of the coil. In order to extend the betatron to higher energy and keep power consumption low enough to run on a continuous basis, it is clearly advantageous to eliminate the air gap. One solution is illustrated in Figure 11.15a. The magnetic flux at the electron orbit is produced by a separate magnet circuit. The beam transport circuit has its own flux-guiding core and magnet windings. The size of the capacitor bank is reduced considerably, and power losses

Betatrons

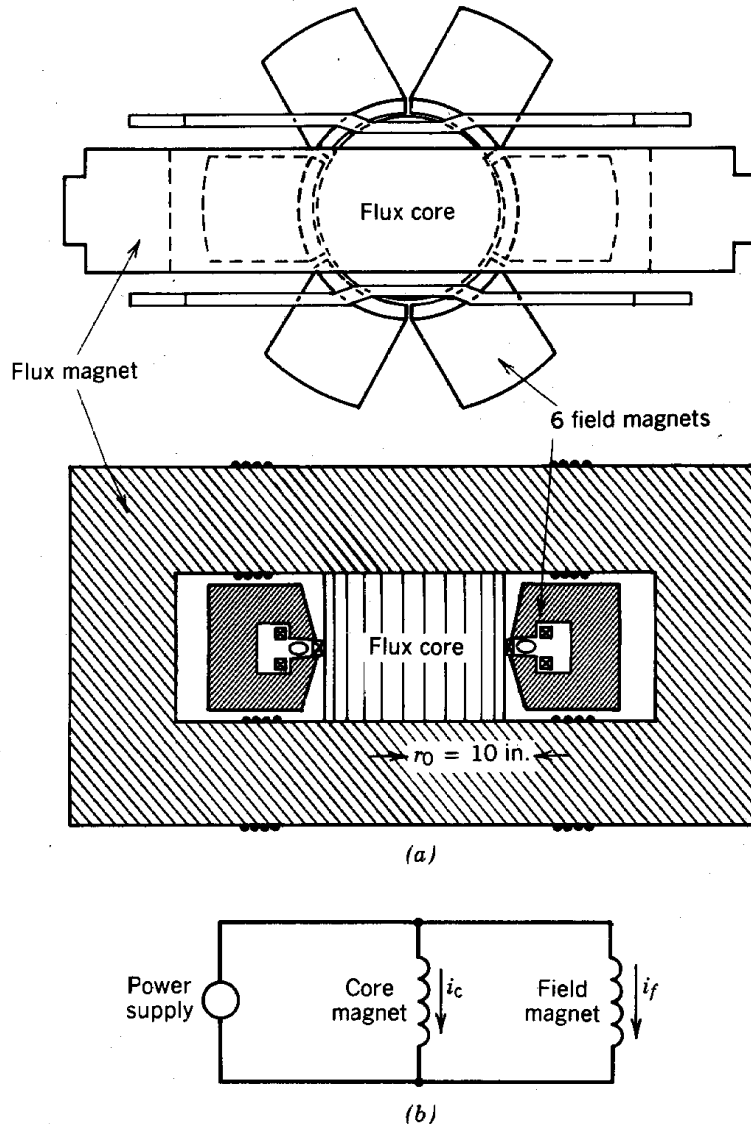


Figure 11.15 High-energy (80-MeV) betatron with no air gap. (a) Geometry of device, showing separate magnet circuits for accelerating flux and bending field. (b) Parallel drive of magnetic circuits guarantees proportionality of magnetic flux. (M. S. Livingston and J. P. Blewett, *Particle Accelerators*, used by permission, McGraw-Hill Book Co.)

are typically only one-third those that would occur with a single-magnet circuit. The disadvantage of the design is the increased complexity of assembly and increased volume of the main circuit core in order to accommodate the bending field circuit.

An interesting problem associated with the betatron of Figure 11.15a is how to drive the two magnetic circuits with close tracking between the transport fields and acceleration flux. An effective solution is to connect both magnets to the same power supply in parallel, as shown in Figure 11.15b. Because the voltage across the windings must be the same, the flux change

Betatrons

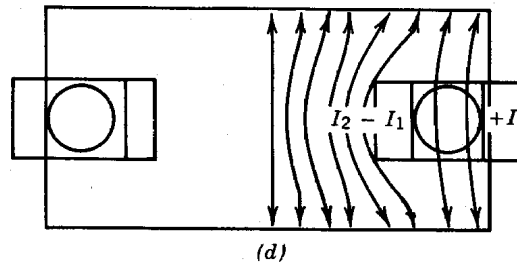
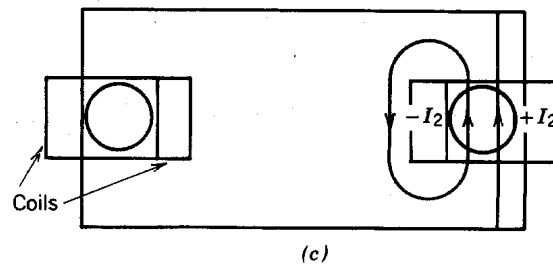
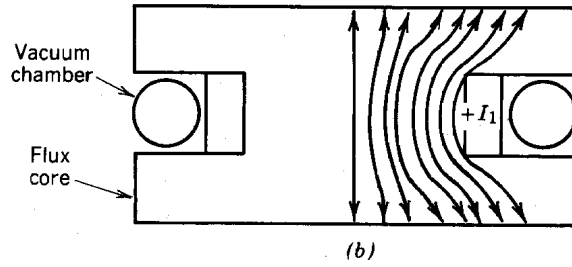
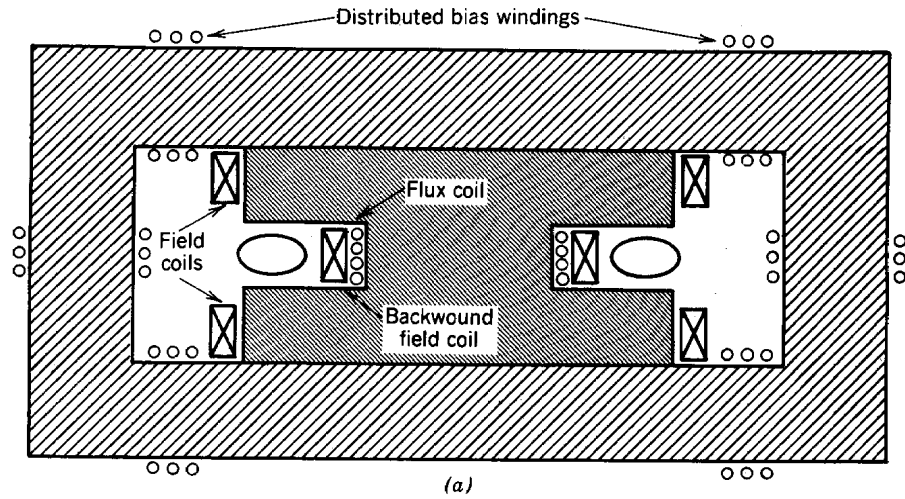
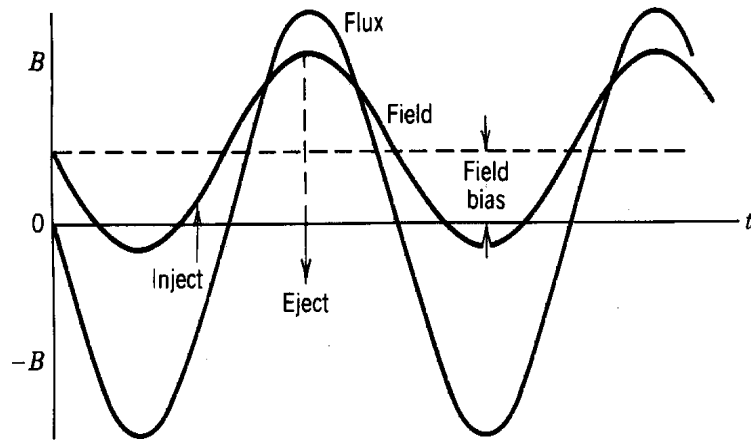
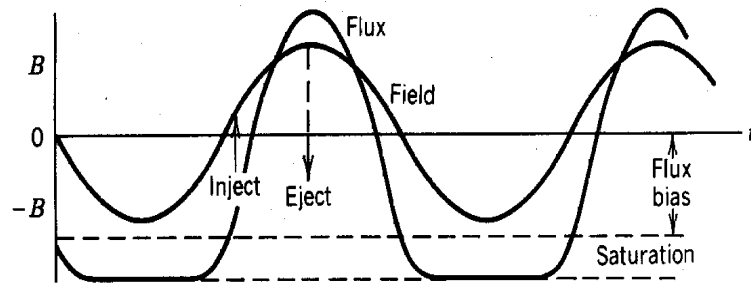


Figure 11.16 Betatron with single magnetic circuit, bias windings, and no air gap. (b) Magnetic field lines in flux core produced by flux winding. (c) Magnetic field lines in flux core and vacuum torus produced by combination of external field coil and backwound field coil. (d) Composite field lines showing accelerating flux and bending field.

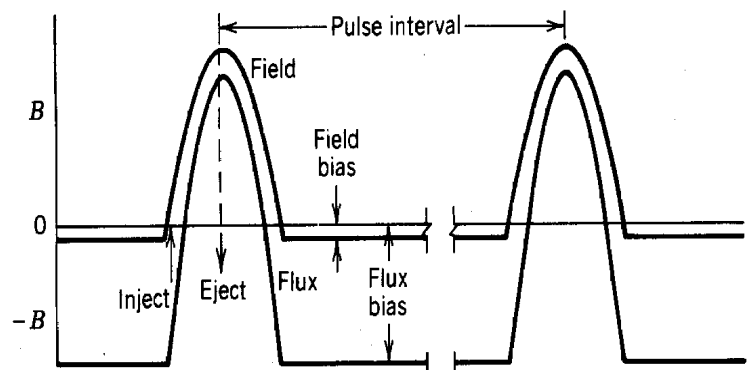
Betatrons



(a)



(b)



(c)

Figure 11.17 Acceleration cycles for high-energy betatrons. Average field inside main orbit and bending field at main orbit plotted versus time. (a) Cycle with field biasing, dc component added to bending field. (b) Cycle with flux biasing and ac power drive; flux core saturated half the time. (c) Cycle of betatron with flux biasing and pulsed power drive from a switched capacitor bank; core must be reset by a separate circuit between each pulse.

Betatrns



Figure 11.18 Betatron for radiation therapy (45 MeV). (a) Photograph of system: accelerator and treatment table. (b) Cross section of accelerator: gamma ray mode (top) and electron beam mode (bottom). (1) Lead shielding. (2) Transformer yokes. (3) Suspension and rotation mechanisms. (4) X-ray target. (5) Central magnet core. (6) Electron guns. (7) X-ray equalizers. (8) Lead shutter. (9) X-ray monitoring system. (10) Collimator. (11) Movable yoke for servicing. (12) Ten scatterer system for electron beam. (13) Electron radiation monitoring system. (14) Variable localizer. (Courtesy BBC Brown, Boveri and Company.)

through both windings is the same. Thus, if the number of turns and geometry of the windings are chosen properly, the ratio of bending field and core flux will be correct throughout the acceleration cycle, independent of the effective μ values in the two cores. This is another application of *flux forcing* (see Section 10.4).

The magnet design of Figure 11.16a represents another stage of improvement. It is much simpler than the magnet of Figure 11.15a and still produces a bending field without an air gap. In order to understand how this configuration works, we shall approach the circuit in parts and then determine the total magnetic field by superposition. First, consider a single coil inside the radius of the vacuum chamber, as shown in Figure 11.16b. All the magnetic flux flows through the central core as shown. In the second stage (Fig. 11.16c), we consider the field produced by a winding inside the vacuum chamber carrying current $-NI$ and a windings outside the chamber carrying current $+NI$. This produces a bending field at the main orbit, and flux returns through the core as shown. In the final configuration, Figure 11.16d, the external windings are present and the windings on the flux coil are reduced by $-NI$ ampere turns to generate the net field. Proper choice of the number of turns on the flux coil versus the field coils plus shunting of the bending field gap assures that the betatron condition is satisfied.

A further improvement to the magnet of Figure 11.16 to reach higher beam energy is to utilize the full available flux swing of the central core during acceleration. In the previous acceleration

Betatrons

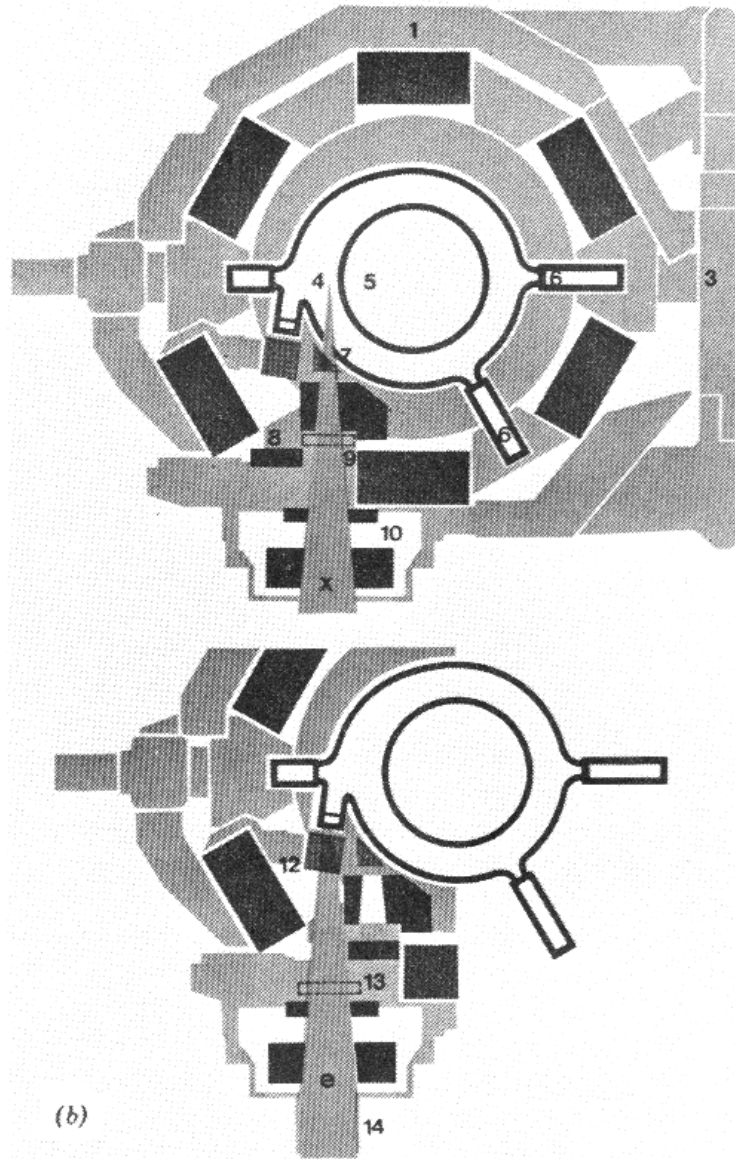


Figure 11.18 (Continued).

cycles we have discussed, the core field changes from 0 to $+B_s$ while the bending field changes from 0 to $+\frac{1}{2}B_s$. Inspection of Eq. (11.13) shows that the betatron condition is expressed in terms of the change of included flux, not the absolute value. An acceleration cycle in which the core magnetic field changes from $-B_s$ to $+B_s$, while the bending field changes from 0 to $+B_s$ satisfies the betatron condition and doubles the final electron energy for a given core size. There are two methods to achieve an acceleration cycle with full flux swing, *field biasing* and *flux biasing*. Field biasing is illustrated in Figure 11.17a. A dc component of magnitude $+\frac{1}{2}B_s$ is added to the bending field. Acceleration takes place over a half-cycle of the ac waveform. For

Betatron

flux biasing, dc bias windings are added to the core circuit to maintain the core at $-B_s$. Bias windings are illustrated in Figure 11.16. The field and flux coils are energized in parallel to produce the accelerating waveform illustrated in Figure 11.17b. Acceleration takes place over one quarter-cycle. The main technological difficulty associated with flux biasing is that the core is driven to saturation, resulting in increased hysteresis and eddy current losses. Also, during the negative half-cycle, the core has $\mu = \mu_0$ so that the circuit inductance varies considerably. Betatrons with flux biasing are usually driven by pulse power modulators rather than resonant circuits. A pulsed acceleration cycle is shown in Figure 11.17c.

A modern commercial betatron for radiation therapy is illustrated in Figure 11.18a. The machine accelerates electrons to a maximum kinetic energy of 45 MeV to generate deeply penetrating radiation. Electrons can be extracted directly or used to generate forward-directed gamma rays on an internal target. The 12,000-kG machine and the treatment table can be moved to a variety of positions to achieve precise dose profiles. A cross section of the betatron (Fig. 11.18b) illustrates operation in the gamma ray and electron modes.